Viser Technology Pte. Ltd.
Mechanical Engineering Science
DOI: 10.33142/mes.v6i1.13223

Research Article Open Access

Research on the Influence of Raceway Waviness on the Vibration Characteristics of Deep Groove Ball Bearings

Yuanlong CHEN, Jiarui ZHOU, Xinyu WEN, Shaoqi WANYAN, Yuqing WANG*

School of Mechanical Engineering, Hefei University of Technology, Hefei, Anhui, 23009, China

***Corresponding Author:** *Yuqing WANG, E-mail: yuqingw@hfut.edu.cn*

Abstract

The dynamics model of a 2-degree-of-freedom deep groove ball bearing is established by incorporating the raceway surface waviness model comprising multiple sinusoidal functions superposition. The model is solved using the fourth-order Runge-Kutta method to obtain the vibration characteristics including displacement, velocity, acceleration, and frequency of the bearing. Validation of the model is accomplished through comparison with theoretical vibration frequencies. The influence of the amplitude of waviness of the inner and outer ring raceway surfaces of deep groove ball bearings on the vibration displacement, peak-to-peak vibration displacement and root-mean-square vibration acceleration is analyzed, and the results show that as the amplitude of the inner and outer ring raceway surfaces waviness increases, all the vibration characteristic indexes increase, indicating that the vibration amplitude of the bearings as well as the energy of the waviness-induced shock waveforms increase with the increase of the amplitude of the waviness.

Keywords: *Waviness; Deep groove ball bearing; Vibration characteristics; Dynamics*

1 Introduction

The deep groove ball bearing serves as a precise component that converts sliding friction into rolling friction, offering benefits such as increased power transmission efficiency and a low coefficient of friction. This type of bearing is widely employed as a fundamental element in rotating machinery [1-2]. In instances where the raceway surface of deep groove ball bearings exhibits defects, the contact force between the rolling element and raceway of the bearings undergoes non-uniform alterations, leading to irregular vibrations and fatigue-related damage. Consequently, delving into the impact of raceway surface imperfections on the vibration properties of rolling bearings holds substantial importance.

Kankar P. K et al [3] conducted a study focusing on examining the impact of the surface waviness of the bearing raceway on the nonlinear vibration characteristics of a bearing rotor system. The research integrated considerations of nonlinear contact stiffness and nonlinear damping occurring between the rolling body and the raceway to gain insights into the system's vibrational behavior. Shah D S et al [4] introduced the changes in bearing stiffness and damping caused by lubricating oil film, and he took into account the mass of shaft, ring, rolling element and shell in modeling, established a mechanical model of the surface waviness of deep groove ball raceway. Sun M et al. [5] used autocorrelation function to simulate the random surface waviness of inner and outer raceways, established a rolling body-raceway contact model considering the surface waviness, and combined it with the theory of acoustic equations, established the computational model of vibration noise of the rolling body and the inner ring. Yang M H et al [6] introduced a different method to solving the Reynolds equation to investigate the effect of different surface waviness parameters of shaft diameter and shaft tile on the static parameters of dynamic compression shaft diameter bearings on the vibration characteristics of the bearings. Liu J et al [7] proposed an enhanced time-varying displacement excitation model for circularity and waviness by using a combination of several sinusoidal functions and improved the dynamics model in the previous study to take into consideration the vibration noise of the rolling element and inner ring including the effect of coupling errors including roundness and corrugation on the bearing vibration characteristics. Tallian T E and Gustafsson O G [8] proposed a dynamical model considering the waviness and investigated the effect of mass and flexibility attached to the bearing on the vibration characteristics. Choudhury A and Tandon N [9] proposed a dynamical model considering free mode and bending vibration of rolling bearings to study the effect of waviness and roller

Received on March 19, 2024; Accepted on April 11, 2024

size deviation on the frequency of rolling bearings. Nizami A [10] developed a computer program to simulate the degree of waviness on the inner and outer rings of rolling bearing raceways and on the surface of rolling elements, investigated the effects of the number of balls, preload, and the degree of waviness on the vibration characteristics of rolling bearings, and verified the correctness of the model by experimental results.

In summary, the surface defects of rolling bearings can be divided into two categories: local defects and distributed defects. Distributed defects include surface roundness, surface waviness, surface roughness and rolling element size deviation, etc., among which the influence of surface waviness amplitude on the vibration characteristics of bearings is less studied. In this work, a reasonable dynamic model of rolling bearing under the excitation of waviness is established by comprehensively considering the corrugation error of the surface of the raceway of the inner and outer rings of rolling bearings. The dynamic model is solved by the fourth-order Runge-Kutta method, and the solution results are compared with the theoretical frequency value to verify the correctness of the established model. Building on this foundation, the research investigates how the amplitude of raceway surface waviness affects the vibration characteristics of rolling bearings.

2 Theoretical Modeling

Different from previous studies, a sinusoidal basis was introduced in this work to characterize the surface waviness of inner and outer raceways, so as to accurately characterize the surface characteristics of inner and outer raceways of rolling bearings under actual working conditions. In contrast to the traditional theoretical research based on the ideal raceway surface model, this work takes the spatial variable curvature surface of the inner and outer raceway and the spatial variable curvature contact surface between the rolling element and the raceway as the starting point, and establishes the theoretical model of surface waviness as shown in Figure 1.

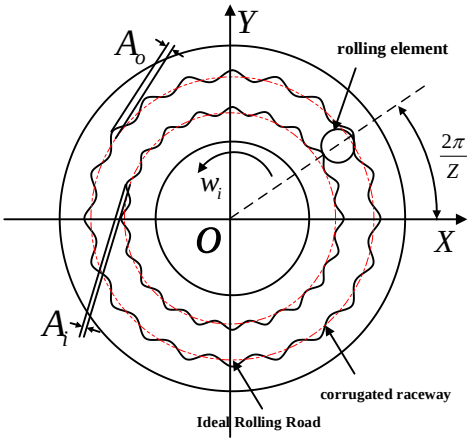

Figure 1 Schematic diagram of sinusoidal basis model of raceway waviness in inner and outer rings

First, the mechanical equations of bearing vibration induced when each roller contacts the outer raceway surface waviness are characterized:

$$T_o = \sum_{s=1}^{k} A_{os} \sin(N_{os}\theta_j + \varphi_{os}) \tag{1}$$

Where A_{os}, N_{os} and φ_{os} denote: the maximum magnitude of the s-order waveform, the wave number, and the initial phase angle, respectively. In addition, the contact angle θ_j between the s-th rolling element and the raceway satisfies the following constraints:

$$\theta_j = \begin{cases} \frac{2\pi}{Z}(j-1) + \omega_c t + \varphi_{0x} & inner \quad ring \\ \frac{2\pi}{Z}(j-1) + (\omega_c - \omega_i)t + \varphi_{0x} & outer \quad ring \end{cases} \tag{2}$$

Where j, Z, w_c, φ_{0x} and w_i denote: the j-th rolling element, the total number of rolling elements, the cage angular velocity, the position angle of the first rolling element relative to the x-axis, and the angular velocity of the inner ring.

By substituting equation (2) into equation (1), the expression of outer ring waviness can be obtained:

$$T_o = \sum_{s=1}^{k} A_{os} \sin\left\{ N_{os}\left[\frac{2\pi}{Z}(j-1) + \omega_c t + \varphi_{ox} \right] + \varphi_{os} \right\} \tag{3}$$

Similarly, the inner ring waviness is characterized as:

$$T_i = \sum_{s=1}^{k} A_{is} \sin\left\{ N_{is}\left[\frac{2\pi}{Z}(j-1) + (w_c - w_i)t + \varphi_{0x} \right] + \varphi_{is} \right\} \tag{4}$$

Secondly, this paper proposes a spring-mass-damping model for rolling bearings by comprehensively considering the change of contact stiffness under the influence of bearing mass, damping and corrugation degree. Figure 2 represents the established dynamic model of deep groove ball bearing. In order to facilitate numerical analysis, the rolling element is uniformly distributed, and the contact between the raceway and the rolling element follows the Hertzian contact theory [11], then the contact between the rolling element and the inner and outer rings is regarded as circular point contacts. Support the plane passing through the center of the rolling body and parallel to the axial plane be the I main plane, and the plane passing through the center of the rolling body and perpendicular to the I main plane be the II main plane, and the contact stiffness K between the raceway and the rolling body can be expressed as:

$$K = \left(\frac{\pi^2 k^2 E^{*2} \Sigma}{4.5 \Gamma^3 \Sigma \rho} \right)^{0.5} \tag{5}$$

Where E^*, $\Sigma\rho$ and k denote: equivalent modulus of elasticity, contact surface curvature sum and elliptic parameters. Moreover, for the full elliptic integrals of

classes I and II Λ and M satisfying:

$$\frac{2}{E^*}=\frac{1-\mu_1^2}{E_1}+\frac{1-\mu_2^2}{E_2} \tag{6}$$

Where $E_1(E_2)$, $u_1(u_2)$ and $\Sigma\rho_I(\Sigma\rho_{II})$ denote: the sum of the modulus of elasticity of the rolling body(raceway) material, the Poisson ratio of the rolling body(raceway) material, and the curvature of the I(II) principal plane.

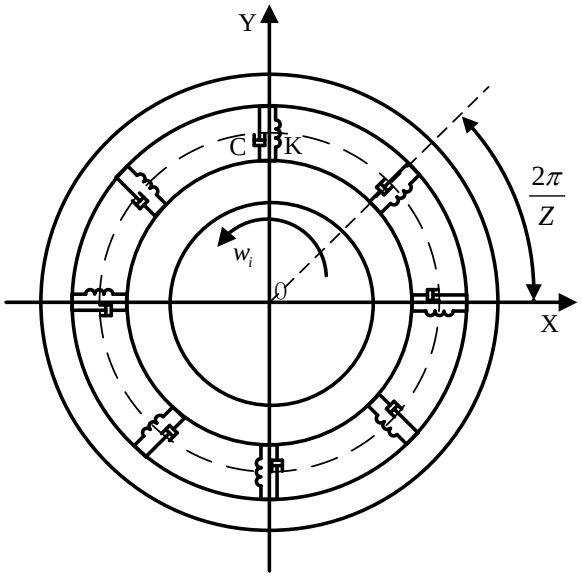

Figure 2 Schematic diagram of the dynamic model of a deep groove ball bearing

Subsequently, the raceway surface in contact with the rolling element is modeled as shown below:

$$\begin{cases} k=1.0339ln\left(\dfrac{\sum\rho_I}{\sum\rho_{II}}\right)^{0.6360} \\ \Lambda=1.5277+0.6023ln\left(\dfrac{\sum\rho_I}{\sum\rho_{II}}\right) \\ M=1.0003+0.5968\left(\dfrac{\sum\rho_{II}}{\sum\rho_I}\right) \end{cases} \tag{7}$$

By integrating equations (5) through (7), one can derive the comprehensive contact stiffness encompassing the interaction between the rolling body and both the inner and outer rings:

$$K=\left(\frac{1}{K_i^n}+\frac{1}{K_o^n}\right)^{-n} \tag{8}$$

Where K_i and K_o denote the contact stiffness of the rolling element with the inner and outer rings. In addition, the deep groove ball bearing load-deflection coefficient n considered in this work is 1.5.

Finally, in view of the rolling bearing operation, the raceway is prone to displacement and deformation of the actual working conditions, the total contact deformation δ_j can be expressed as:

$$\delta_j=x\cos\theta_j+y\sin\theta_j-\gamma+T_i+T_o \tag{9}$$

Where $x(y)$ and γ is the displacement and radial clearance of the inner ring in the $X(Y)$ direction. The contact coefficient S_j is introduced to characterize the difference between the loaded and unloaded areas of the raceway:

$$S_j=\begin{cases}1, & \delta_j>0\\ 0, & \delta_j\le 0\end{cases} \tag{10}$$

Development of a two-degree-of-freedom rolling bearing dynamics model to describe bearing vibration characteristics under waviness excitation:

$$\begin{cases} m\ddot{x}+c\dot{x}+\sum_{j=1}^{z}KS_j(x\cos\theta_j+y\sin\theta_j-\gamma+T_i+T_o)^n\cos\theta_j=F_x \\ m\ddot{y}+c\dot{y}+\sum_{j=1}^{z}KS_j(x\cos\theta_j+y\sin\theta_j-\gamma+T_i+T_o)^n\sin\theta_j=F_y \end{cases} \tag{11}$$

Where m, c and $F_x(F_y)$ denote: the mass of the inner ring and the supporting shaft, the internal damping coefficient of the bearing, and the radial force of the bearing in the direction of the $X(Y)$ axis.

3 Numerical Algorithm

Based on equations (1)-(11), this work takes deep groove ball bearing 6308 as the entry point to analyze the influence mechanism of raceway waviness degree on bearing vibration characteristics. Its basic geometric parameters are shown in Table 1.

Table 1 Geometric dimensions of 6308 deep groove ball bearings

Physical parameter	Operator	Dimension	Value
Inner ring diameter	D_{in}	mm	40
Diameter of outer ring	D_{out}	mm	90
Rolling body pitch diameter	D	mm	65
Number of scrollers	Z	\	8
Contact angle	θ	°	0
Rolling body diameter	d	mm	15.081
Inner ring raceway diameter	D_i	mm	80.088
Outer ring raceway diameter	D_o	mm	49.912

Take the mass of the inner ring of the rolling bearing $m=0.6kg$, damping coefficient $c=200Ns\cdot m^{-1}$ and bearing speed $N_s=2000r\cdot\min^{-1}$. Solve the dynamics equation of equation (13) using the fourth-order Runge-Kutta method with a time step $\Delta t=5\times10^{-6}s$. It's assumed that the initial displacement of the system $x_0=y_0=10^{-6}m$ and the initial velocity $\dot{x}_0=\dot{y}_0=0$. The corresponding algorithmic flowchart for numerical computation is shown in Figure 3.

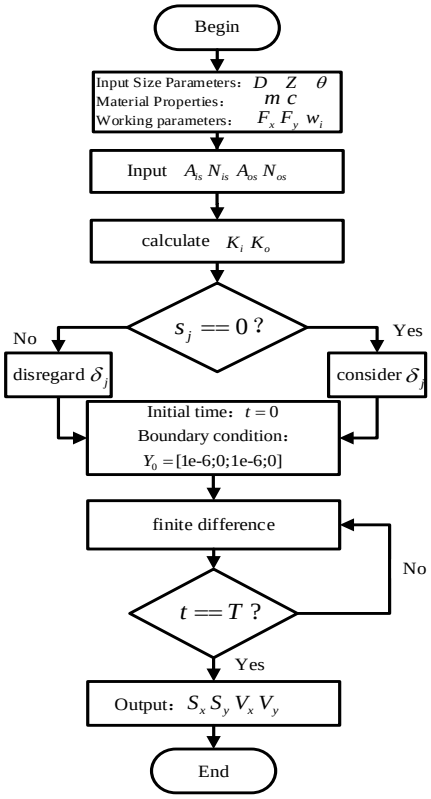

Figuer 3 Algorithm flowchart

4 Vibration Characterization Analysis

4.1 Solution of dynamic equations

In this paper, the basic size parameters, initial load and speed of the rolling bearing are input first. Secondly, according to the established waviness model, input parameters such as the amplitude and wave number of the raceway waviness. Then, the contact stiffness between the rolling element and the inner and outer rings of the raceway is calculated. Finally, the four-order Runge-Kutta method was used to calculate the dynamics model of 2 degrees of freedom. At the end of the iteration, the displacement, velocity and acceleration curves of the inner ring of the rolling bearing on the x and y axes were output, as shown in Figure 4.

4.2 Model verification

4.2.1 Verification of vibration characterization

The displacement curves along the x-axis and y-axis were subjected to Fourier transformation to generate the displacement frequency domain representation of the bearing in both the x-axis and y-axis orientations, as illustrated in Figure 5.

The results presented in Figure 4 (a) - (f) indicate a noticeable periodicity in the vibration displacement, velocity, and acceleration of the inner ring of the rolling bearing in the time domain waveform. This behavior is attributed to the alternating odd and even number of balls in the load region of the ball bearing under radial force influence, leading to vibrations of the bearing with the outer ring at specific frequencies. Further observation of Figure 5 shows that the inner ring of the bearing in the x-axis direction and the y-axis direction are in the 103.3Hz at the obvious peak, and the corresponding conditions listed in Table 2 of the ball bearing outer ring through the frequency of 102.4Hz is basically consistent with the establishment of the model is correct.

Table 2 6308 deep groove ball bearings at various frequencies at $2000r \cdot \min^{-1}$

Rolling body rotation frequency f_{bs}	Cage rotation frequency f_c	Outer Ring Passing Frequency f_{bpo}	Inner Circle Passing Frequency f_{bpi}
70.0Hz	12.8Hz	102.4Hz	164.3Hz

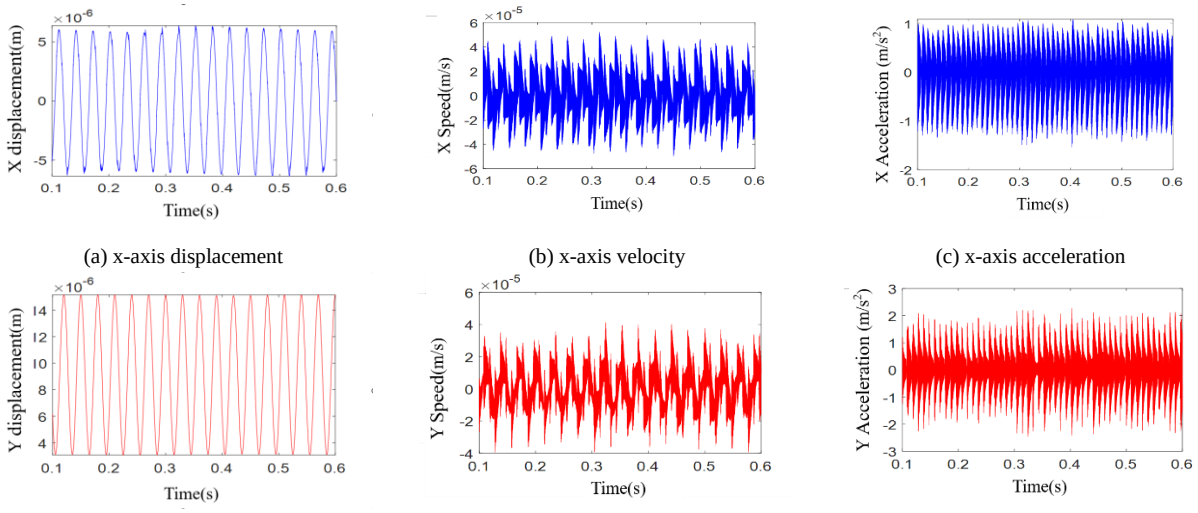

(a) x-axis displacement (b) x-axis velocity (c) x-axis acceleration

(d) y-axis displacement (e) y-axis velocity (f) y-axis acceleration

Figure 4 Vibration displacement, velocity and acceleration curves of the inner ring of the bearing

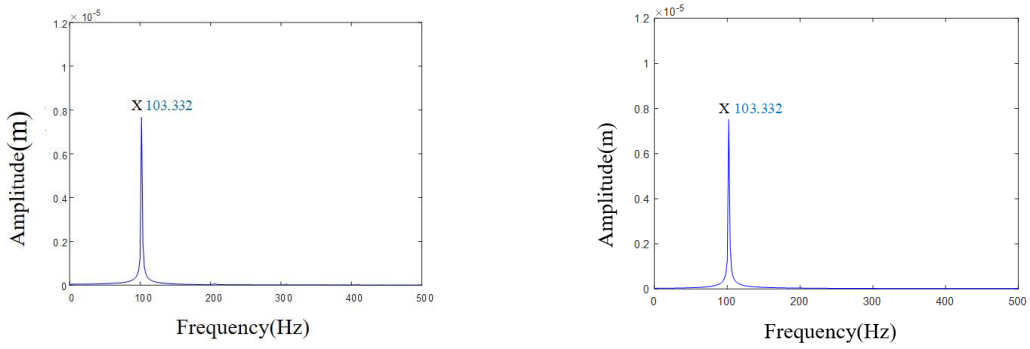

(a) x-axis direction (b) y-axis direction

Figure 5 Spectrogram of vibration displacement of the inner ring of the bearing

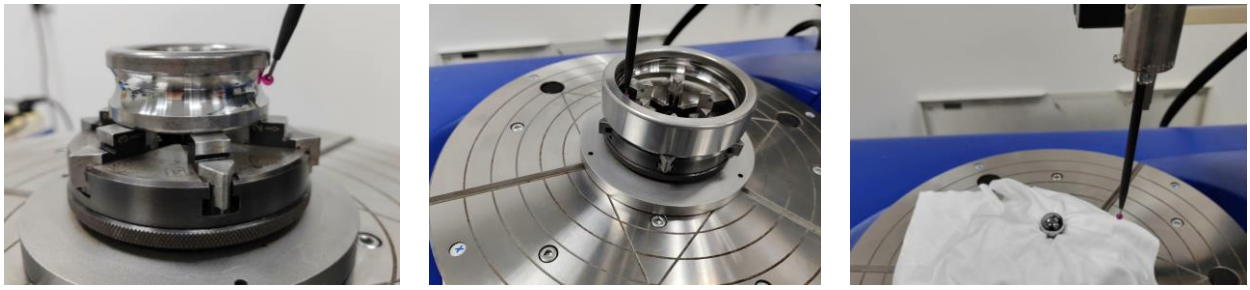

(a) internal raceway (b) outer raceway (c) rolling element

Figure 6 Waviness measurement of 6308 deep groove ball bearing

4.2.2 Verification of waviness model

The waviness model proposed in this study is a composite of sine functions with varying amplitudes and wave numbers. To validate the accuracy of the established model, a waviness test was conducted on a 6308 deep groove ball bearing using an MMD-100JS profilometer. The measurement points are illustrated in Figure 6.In order to ensure accuracy in the measurement test, three measurements were conducted for each part, and the average value of the three measurement results was utilized for data analysis. Taking the waviness of the inner raceway surface as an example, this data was analyzed.

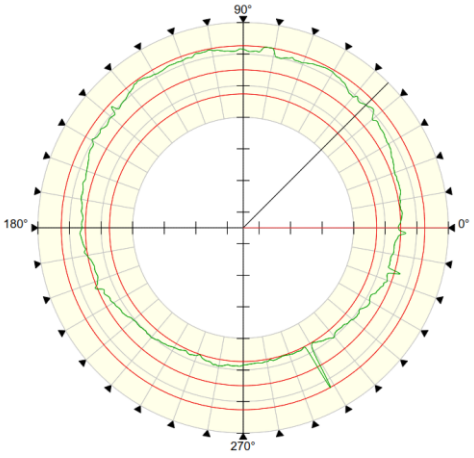

Figure 7 Waviness error diagram of the inner ring

The computer system employs the minimum region method for roundness error calibration to evaluate and present the measurement results graphically, as depicted in Figure 7.

Harmonic analysis of the measurement results, take 4-100upr data, get 6308 deep groove ball bearing inner ring raceway waviness error of the harmonic analysis of the data as Table 3, Figure 8 shows.

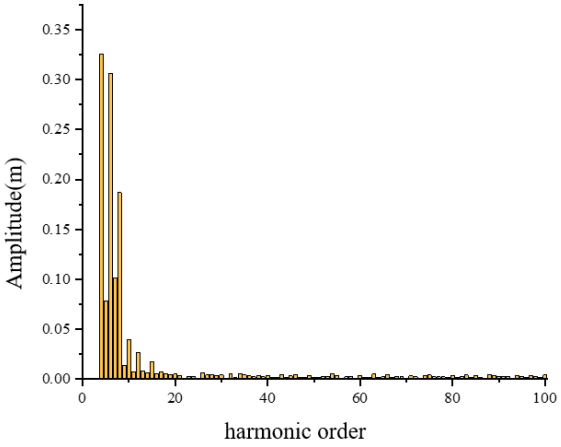

Figure 8 Histogram of waviness harmonic analysis of inner ring

The results of the harmonic analysis reveal that the waviness of the inner ring in the rolling bearing is formed through the superposition of sine functions with varying amplitude and frequency. This finding aligns with the established waviness model, thereby confirming its accuracy.

Table 3 Inner raceway harmonic analysis data (4-100upr)

UPR	N+0	N+1	N+2	N+3	N+4	N+5	N+6	N+7	N+8	N+9
0				0.3256	0.0784	0.3065	0.1012	0.1869	0.014	0.0394
10	0.0075	0.0271	0.0085	0.0065	0.0178	0.0052	0.007	0.0057	0.0045	0.005
20	0.0036	0.0006	0.0028	0.0027	0.0012	0.0065	0.0045	0.0049	0.0037	0.0045
30	0.0009	0.0055	0.0018	0.0057	0.0043	0.0033	0.0023	0.004	0.0024	0.0038
40	0.0018	0.0022	0.0046	0.0019	0.0033	0.0044	0.0017	0.0016	0.004	0.0014
50	0.0021	0.0029	0.0024	0.0052	0.0038	0.0004	0.0023	0.003	0.0009	0.0033
60	0.0018	0.0019	0.0053	0.0019	0.0025	0.0046	0.0022	0.003	0.0031	0.001
70	0.0034	0.0025	0.0011	0.0039	0.0044	0.0025	0.0024	0.0023	0.0019	0.0041
80	0.0022	0.0025	0.0043	0.0017	0.0039	0.0021	0.0013	0.0042	0.0035	0.0029
90	0.0029	0.003	0.0011	0.0036	0.0026	0.0022	0.0035	0.0027	0.0022	0.0043

4.3 Influence of waviness amplitude on vibration characteristics of deep groove ball bearings

Taking the bearing radial load $F_x = 0$, $F_y = 20N$, radial clearance $C_y = 1um$, waviness number 7, and bearing speed $N_s = 2000r \cdot \min^{-1}$ as the working condition, the influence of raceway surface waviness amplitude on bearing vibration displacement, peak-to-peak value of vibration displacement and root mean square value of acceleration was analyzed.

4.3.1 Inner ring

The vibration displacement curve of the bearing in the y-axis direction is shown in Figure 9 when the inner ring ripple amplitude is 0.2um, 0.4um, 0.8um and 1.2um. From Figure 9, it can be seen that the vibration displacement of the rolling bearing in the y-axis direction increases with the increase of the amplitude of the inner ring waviness. The relationship between the inner ring waviness amplitude and the peak-to-peak value of the bearing vibration displacement in the y-axis direction is shown in Figure 10. Analysis of Figure 10 reveals a direct relationship between the peak-to-peak value of the vibration displacement in the y-axis direction of the bearing and the inner ring waviness amplitude, indicating that the former increases proportionally with the latter.

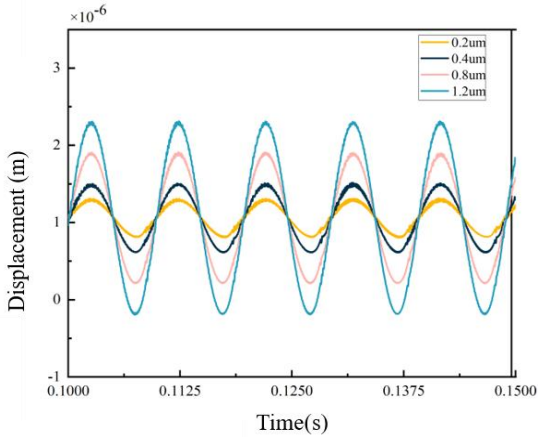

Figure 9 The influence of the waviness amplitude of the inner ring on the vibration displacement in the y-axis direction of the bearing

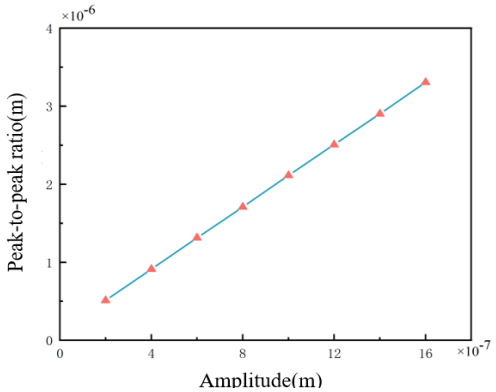

Figure 10 The influence of the waviness amplitude of the inner ring on the vibration displacement in the y-axis direction of the bearing

Root mean square (RMS), referred to as the root mean square or effective value [12], is commonly used to represent the effective value of a physical quantity. In this paper, the RMS value of the vibration acceleration of the bearing is used to represent the energy of the impact waveform induced by waviness, and its expression is as follows:

$$RMS_a = \sqrt{\frac{1}{N}\sum_{i=1}^{N} a_i^2} \tag{14}$$

Where a_i denote the i-th acceleration data, N denotes the total number of acceleration data to be analyzed

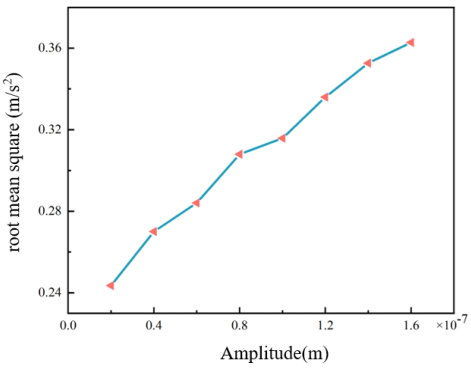

Figure 11 The effect of the waviness amplitude of the inner ring on the RMS value of vibration acceleration in the y-axis direction of the bearing

Figure 11 depicts the correlation between the amplitude of inner ring waviness and the root mean square (RMS) value of vibration acceleration along the y-axis of the bearing. The graphical suggests a direct relationship between the vibration acceleration's RMS value in the bearing shaft direction and the inner ring waviness amplitude. As the amplitude of inner ring waviness escalates, the RMS value of vibration acceleration also rises, indicating a corresponding increase in the impact waveform energy caused by the waviness.

4.3.2 Outer ring

The vibration displacement curve of the bearing in the y-axis direction is depicted in Figure 12 for varying amplitudes of outer ring waviness, specifically at 0.2um, 0.4um, 0.8um and 1.2um. Analysis of Figure 12 reveals a direct correlation between the amplitude of the outer ring waviness and the vibration displacement of the rolling bearing along the y-axis direction, indicating that as the outer ring waviness amplitude increases, so does the vibration displacement.

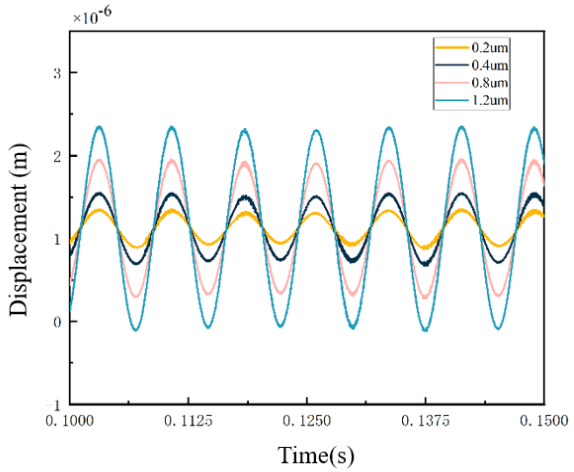

Figure 12 The influence of the waviness amplitude of the outer ring on the vibration displacement in the y-axis direction of the bearing

The relationship between the outer ring waviness amplitude and the peak-to-peak value of vibration displacement in the y-axis direction of the bearing is shown in Figure 13. From Figure 13, it can be seen that the peak-to-peak value of the vibration displacement of the bearing in the y-axis direction is positively correlated with the magnitude of the outer ring waviness, and the peak-to-peak value of the vibration displacement in the y-axis direction of the bearing increases with the increase in the magnitude of the outer ring waviness. The relationship between the outer ring waviness amplitude and the root-mean-square value of the vibration acceleration in the y-axis direction of the bearing is shown in Figure 14. It can be seen from Figure 14 that the RMS value of the vibration acceleration in the y-axis direction of the bearing is positively correlated with the amplitude of the outer ring waviness and increases with the increase of the amplitude of the outer ring waviness, indicating that with the increase of the amplitude of the outer ring waviness, the energy of shock waveforms triggered by the waviness increases subsequently.

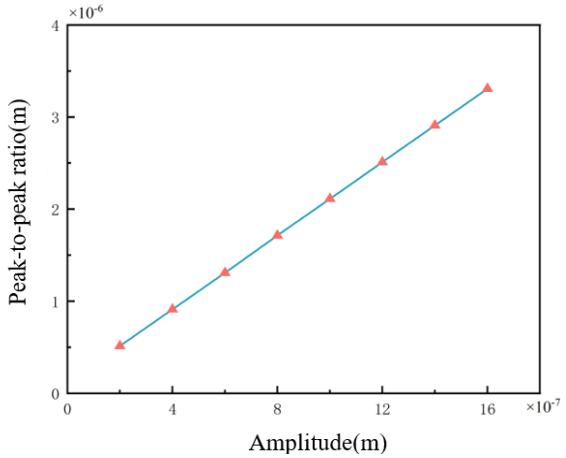

Figure 13 The effect of the waviness amplitude of the outer ring on the peak-to-peak value of the vibration displacement in the y-axis direction of the bearing

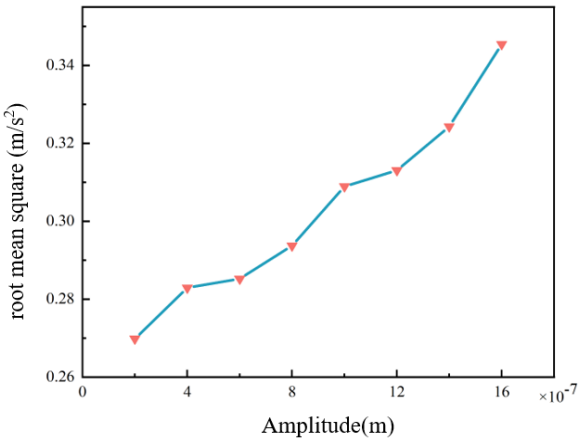

Figure 14 The influence of the waviness amplitude of the outer ring on the RMS value of vibration acceleration in the y-axis direction of the bearing

5 Conclusion

Different from previous studies, this work focuses on exploring the key scientific problems of deep groove ball bearing damage dynamic mechanism mining and the key technical problems of deep groove ball bearing dynamic optimization control that urgently need to be solved in the RV reducer production industry. Taking 6308 deep groove ball bearing as the research entry point, a sinusoidal based raceway surface waviness model is established. The dynamic model of 2-degree-of-freedom deep groove ball bearing was improved, and the numerical solution of the characteristic dynamic parameters of the model was obtained by using the fourth-order Runge-Kutta algorithm. The relevant findings are summarized below:

(1) As the waviness amplitude of the raceway surface and outer ring increases, the vibration displacement of the bearing inner ring in the y-axis direction and the peak-to-peak value of vibration displacement increase, that is, the bearing vibration amplitude increases with the increase of the waviness amplitude of raceway surface.

(2) The vibration acceleration value of the bearing inner ring in the y-axis direction increases with the increase of waviness amplitude of the raceway surface and outer ring surface, that is, the energy of impact waveform induced by waviness increases with the increase of waviness amplitude of raceway surface.

Finally, the development of this research work contributes to digging deeper into the precision bearing processing raceway surface accuracy induced by the heterogeneous irregular waviness on the bearing vibration characteristics of the influence of the law, helps to explore the harsh operating conditions of the bearing running state real-time health monitoring to provide a certain degree of scientific reference and engineering reference.

References

[1] Yu G, Su M, Xia W, et al. Vibration characteristics of deep groove ball bearing based on 4-DOF Mathematical Model[J]. Procedia Engineering, 2017(174):808-814.

[2] Zhi-Jie J, Bin Z, You-Liang Z, et al. Analysis of the miniature deep groove ball bearing radial clearance loaded measuring method[J]. Journal of Mechanical & Electrical Engineering, 2015,32(2):223-227.

[3] Kankar P K, Sharma S C, Harsha S P. Nonlinear vibration signature analysis of a high speed rotor bearing system due to race imperfection[J]. Journal of Computational and Nonlinear Dynamics, 2012 (1):11014.

[4] Shah D S, Patel V N. Theoretical and experimental vibration studies of lubricated deep groove ball bearings having surface waviness on its races[J]. Measurement, 2018(129):405-423.

[5] Sun M, Xu H, An Q. Noise calculation method of deep groove ball bearing caused by vibration of rolling elements considering raceway waviness[J]. Proceedings of the Institution of Mechanical Engineers, Part C: Journal of Mechanical Engineering Science, 2021,236(8):4429-4439.

[6] Yang M, Lu H, Zhang X, et al. Influence of surface waviness of journal and bearing bush on the static characteristics of hydrodynamic bearing[J]. Processes, 2021, 9(1):110.

[7] Jing L, Ruikun P, Yajun X U, et al. Vibration analysis of a single row angular contact ball bearing with the coupling errors including the surface roundness and waviness[J]. Science China: Technological Sciences, English Edition, 2020,63(6):10.

[8] Tallian T E, Gustafsson O G. Progress in rolling bearing vibration research and control[J]. A S L E Transactions, 1965,8(3):195-207.

[9] Choudhury A, Tandon N. A theoretical model to predict vibration response of rolling bearings to distributed defects under radial load[J]. Journal of vibration and acoustics: Transactions of the ASME, 1998 (1):120.

[10] Aktu Rk N. The effect of waviness on vibrations associated with ball bearings[J]. Journal of Tribology, 1999(9):45-48.

[11] Li H, Du G. Characterization of radial stiffness of high-speed deep groove ball bearings considering elastic flow lubrication[J]. Bearing, 2021(10):10-13+19.

[12] Yong C, Li X. Research on the conversion method of effective value between vibration acceleration, velocity and displacement[J]. Light Industry Science and Technology, 2024,40(1):70-72.